aval Research Laboratory
shington, DC 20375-5000

NRL/MR/4790—92-6954

Nonlinear Analysis of a Grating Free-Electron Laser

B. HAFIZI,* P. SPRANGLE, AND P. SERAFIM†

Beam Physics Branch
Plasma Physics Division

**Icarus Research*
7113 Exfair Rd.
Bethesda, MD 20814

†*Northeastern University*
Boston, MA 02115

March 31, 1992

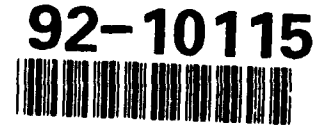

REPORT DOCUMENTATION PAGE

Form Approved
OMB No. 0704-0188

1. AGENCY USE ONLY *(Leave blank)*	2. REPORT DATE	3. REPORT TYPE AND DATES COVERED
	March 31, 1992	Interim March 31, 1992

4. TITLE AND SUBTITLE

Nonlinear Analysis of a Grating Free-Electron Laser

5. FUNDING NUMBERS

6. AUTHOR(S)

B. Hafizi,* P. Sprangle, and P. Serafim†

7. PERFORMING ORGANIZATION NAME(S) AND ADDRESS(ES)

Naval Research Laboratory
Washington, DC 20375-5000

8. PERFORMING ORGANIZATION REPORT NUMBER

NRL/MR/4790—92-6954

9. SPONSORING/MONITORING AGENCY NAME(S) AND ADDRESS(ES)

DARPA
Arlington, VA 22203

10. SPONSORING/MONITORING AGENCY REPORT NUMBER

11. SUPPLEMENTARY NOTES

*Icarus Research, Bethesda, MD 20814
†Northeastern University, Boston, MA 02115

12a. DISTRIBUTION/AVAILABILITY STATEMENT

Approved for public release; distribution unlimited.

12b. DISTRIBUTION CODE

13. ABSTRACT *(Maximum 200 words)*

A two-dimensional nonlinear model of a grating free-electron laser is formulated that includes the effects of self-field forces, finite beam emittance, energy spread and gyromotion of electrons in a guide magnetic field. The start-oscillation current and energy spread requirement for operation at either 100 μm or at 10μm are determined. The designs call for mildly relativistic ($\leq 1/2$ MV) electron beams. The extraction efficiency is determined by numerical simulation. Three different examples are studied in order to elucidate the nonlinear stage of the interaction. We analyze the examples of an infinitely-thin beam, a finite-thickness beam with laminar flow and a finite-thickness beam with full transverse motion. For a thick beam we find the interesting result that the effect of electron gyration about the beam axis is to enhance the extraction efficiency as compared to that for a beam with laminar flow. The numerical results for the extraction efficiency are found to be in close agreement with analytical estimates based on a model in which the electrons are trapped in the slow-wave associated with the grating structure.

14. SUBJECT TERMS

Grating free electron laser
Extraction efficiency
Beam emittance
Start-oscillation current
Infra-red radiation
Moderate energy electron beam

15. NUMBER OF PAGES 34

16. PRICE CODE

17. SECURITY CLASSIFICATION OF REPORT	18. SECURITY CLASSIFICATION OF THIS PAGE	19. SECURITY CLASSIFICATION OF ABSTRACT	20. LIMITATION OF ABSTRACT
UNCLASSIFIED	UNCLASSIFIED	UNCLASSIFIED	SAR

CONTENTS

NONLINEAR ANALYSIS OF A GRATING FREE-ELECTRON LASER

I. Introduction

In a conventional free-electron laser (FEL) the radiation wavelength is given by $\lambda = \lambda_w/2\gamma_z^2$, where λ_w is the wiggler period and $\gamma_z = (1-v_z^2/c^2)^{-1/2}$ is the relativistic mass factor associated with the axial electron velocity v_z. Based on this formula the operation of a conventional FEL in the IR region of the spectrum necessitates the use of multi-MV electron beams. In practice, for voltages in excess of 1 MV the accelerator and the attendant shielding represent a large fraction of the cost and bulk of a FEL. Consequently, alternative sources of IR (and shorter wavelength) radiation are under consideration in a number of laboratories. An example of this is a free-electron source of radiation based on the Smith-Purcell mechanism.[1] In this device an electron beam is made to pass in close proximity of the surface of a metallic grating. Interaction of the electron beam with the slow-wave structure of the grating leads to bunching of the beam and amplification of radiation.[2-20] Since only moderate energy ($<$ few MeV) electron beams are required, the grating FEL has the potential of developing into a truly compact, table-top source of IR radiation.

At the Naval Research Laboratory a grating FEL experiment is underway whose ultimate goal is the generation of high-power radiation in the near-IR windows in the atmosphere. A key element of this experiment is the use of state-of-the-art, high-brightness electron beams obtained from novel cathode materials and designs.

A schematic of the experimental set-up, also known as the orotron configuration[2], is shown in Fig. 1. A virtue of this configuration is that the electron beam may be

Manuscript approved February 14, 1992.

made to interact with a spatial harmonic whose group velocity is nearly zero and consequently the energy drained from the radiation field is reduced. This is illustrated in Fig. 2 which indicates schematically one of the infinite set of dispersion curves for an open resonator formed by two reflecting surfaces, one of which is a plane mirror and the other is a periodic slow-wave structure such as a grating.

In this paper we shall formulate a nonlinear model of a grating FEL with allowance for electron beam emittance and gyromotion in a guide magnetic field. We shall make use of the model to obtain design parameters for experiments aimed at the generation of 100 μm and of 10 μm radiation using mildly relativistic ($\leq 1/2$ MV) electron beams. The nonlinear extraction efficiency is determined by means of numerical simulation of the grating FEL. A principal objective of this paper is to explore the nonlinear stage of the interaction. To elucidate the nature of the saturation mechanism, we shall describe in detail the simulation results for the examples of an infinitely-thin beam, a finite-thickness beam with laminar flow and a finite-thickness beam with full transverse motion. It is found that, for a thick beam, electron gyration leads to an enhancement of the extraction efficiency as compared to the case with laminar electron flow. Assuming that at saturation the electrons are trapped in the slow-wave structure of the grating, we obtain analytical estimates for the efficiency which are in close agreement with the the numerical results.

There are trade-offs in utilizing a mildly relativistic ($\leq 1/2$ MV) beam to generate radiation by a grating FEL. To point out some of these, an example of 10 μm radiation generated by a 5 MV beam is briefly discussed in the last section.

II. Nonlinear Formulation

In this section we shall derive a set of equations that describe the motion the electrons in the electromagnetic field inside the open resonator and in the presence of an axial magnetic guide field. The orientation of the coordinate axes is indicated in Fig. 1, with the origin of coordinates chosen such that the grooves in the grating lie in the region $x < 0$. Region I denotes the space above the grating surface and bounded by the upper mirror and region II denotes the space in the grating slots, i.e, $x < 0$. It is assumed that the interaction of electrons with the z component of the electric field is the dominant mechanism for amplification of the electromagnetic field. Consequently, only TM modes will be considered herein. The dependence of the fields on the y coordinate is assumed to be negligible.

A. Resonator Field

The z component of the resonator electric field can be written as

$$\mathcal{E}_z(x,z,t) = E_z(x,z)\exp(-i\omega t) + c.c., \tag{1}$$

where $\omega = 2\pi c/\lambda$ is the frequency, λ is the free-space wavelength and $E_z(x,z)$ represents the spatial variation of the field. In region I, E_z is expressible as a sum of all the even spatial harmonics representing TM_{l0n} modes:

$$E_z(x,z) = E_0 \sin[k_x(D-x)] + \sum_{n=1}^{\infty} E_n \cos(2\pi\, n\, z/d)\, \sinh[k_n(D-x)], \tag{2}$$

where d is the grating period and D is the distance between the upper surface of the grating and the upper mirror. In Eq. (1), E_0 is the amplitude of the $n = 0$

(i.e., fundamental) spatial harmonic, with wavenumber k_x and E_n is the amplitude of the nth spatial harmonic, with wavenumber k_n. The wavenumbers k_x and k_n will be identified in the following.

In order to simplify the analysis it will be assumed herein that in region II the field corresponds to that of a TEM standing wave in each slot:

$$E_z(x) = A_0 \frac{\sin[k_x(x+b)]}{\sin(k_x b)}, \tag{3}$$

where b is the depth of each groove. The assumption of a TEM mode in region II is strictly valid for $s \ll d$, where s is the groove width.

In writing Eqs. (2) and (3) the fields have been expressed in such a way as to automatically satisfy the boundary condition $E_z = 0$ at the metallic boundaries, i.e. at the bottom of each slot and at the surface of the upper mirror. The other relevant components of the electromagnetic field (i.e., B_y and E_x) may be obtained from Maxwell's equations. It follows from the wave equation that $k_x = \omega/c$ and

$$k_n = \left[(2\pi n/d)^2 - (\omega/c)^2\right]^{1/2}, \quad (n = 1, 2, 3, ...).$$

From the continuity condition on E_z one obtains

$$E_n = 2E_0 \frac{\sin(\pi n s/d)}{\pi n s/d} \frac{\sin(k_x D)}{\sinh(k_n D)}, \tag{4}$$

and from the continuity condition on B_y one obtains the dispersion relation

$$\cot(k_x D) = -\frac{d}{s}\cot(k_x b) + 2\sum_{l=1}^{\infty} \frac{k_x}{k_l} \coth(k_l D) \left[\frac{\sin(\pi l s/d)}{\pi l s/d}\right]^2. \tag{5}$$

In the following it will be assumed that only the $n = 1$ spatial harmonic is resonant with the electrons and therefore the only relevant component of the slow-wave structure. That is, $\lambda/d \approx 1/\beta_z$, where $\beta_z = v_z/c$ is the ratio of the axial electron velocity to the speed of light. All other spatial harmonics are assumed to be nonresonant.

B. Trajectories, Beam Emittance and Energy Spread

The equations of motion of the jth electron, of charge $-|e|$ and rest mass m, interacting with the $n = 1$ spatial harmonic represented in Eq. (2) are given by

$$\frac{d\psi_j}{dt} = 2\pi c\beta_{zj}/d - \omega, \tag{6}$$

$$\frac{d\gamma_j}{dt} = -\frac{|e|E_1\beta_{zj}}{2mc}\sinh[k_1(D - x_j)]\exp(i\psi_j) + c.c., \tag{7}$$

where $\psi_j = 2\pi z_j/d - \omega t$.

To analyze the motion of electrons in the $x - y$ plane it will be assumed that the motion in this plane is unaffected by the radiation field. The forces in the transverse plane arise from the self-electric and the self-magnetic fields plus that due to the axial guide magnetic field, B_0. For a strip beam the equations of motion of an electron are

$$\frac{d^2x}{dt^2} - \Omega_b^2 x = -\Omega_0\frac{dy}{dt}, \tag{8}$$

$$\frac{d^2y}{dt^2} = \Omega_0\frac{dx}{dt}, \tag{9}$$

where $\Omega_0 = |e|B_0/\gamma mc$ is the relativistic gyrofrequency in the guide field, $\gamma = (1 - v^2/c^2)^{-1/2}$, $\Omega_b = (4\pi n_b|e|^2/\gamma\gamma_z^2 m)^{1/2}$ is the relativistic plasma frequency and

n_b is the beam density. We assume herein that the electrons are emitted from the surface of a field-free cathode with no velocity along the y axis. Therefore, setting the canonical momentum equal to zero, i.e., $P_y = \gamma m(dy/dt - \Omega_0 x) = 0$, Eq. (8) simplifies to

$$\frac{d^2x}{dt^2} + \Omega^2 x = 0, \tag{10}$$

where $\Omega^2 = \Omega_0^2 - \Omega_b^2$. To solve Eq. (10) we put[22]

$$x(t) = \xi X(t) \exp[i\phi(t) + \theta], \tag{11}$$

and substitute in to obtain equations for $X(t)$ and $\phi(t)$. It must be emphasized that in Eq. (11) X and ϕ are the same for all the electrons and that $0 \leq \xi \leq 1$ and $0 \leq \theta \leq 2\pi$ are parameters that may be chosen to represent any desired distribution of electrons. The equations for X and ϕ are

$$\frac{d^2X}{dt^2} - X\left(\frac{d\phi}{dt}\right)^2 + \Omega^2 X = 0, \tag{12}$$

$$X^2 \frac{d\phi}{dt} = \epsilon v_z. \tag{13}$$

In Eq. (13) ϵ is a constant that may be shown to equal the beam emittance as follows. Examination of Eq. (11) reveals that the trajectories in the plane $(x, dx/dt)$ are elliptical, with a maximum area of $\pi\epsilon v_z$. This allows one to immediately identify ϵ as the (unnormalized) emittance of the electron beam and Eq. (12) then takes the form of the well-known envelope equation[22]:

$$\frac{d^2X}{dt^2} + \Omega^2 X - \frac{\epsilon^2 v_z^2}{X^3} = 0. \tag{14}$$

For a matched electron beam $X(t) = X_b$ = constant and Eq. (14) may be solved to obtain $X_b = (\epsilon v_z/\Omega)^{1/2}$. Making use of this, the motion in the $x - y$ plane is found to be given by

$$x = \xi \left(\frac{\epsilon v_z}{\Omega}\right)^{1/2} \cos(\Omega t + \theta), \tag{15}$$

$$y = \xi \frac{\Omega_0}{\Omega} \left(\frac{\epsilon v_z}{\Omega}\right)^{1/2} \sin(\Omega t + \theta). \tag{16}$$

It is convenient to relate the half-width of the electron beam, $X_b = (\epsilon v_z/\Omega)^{1/2}$, to the effective spread in the axial energy on the beam, $< \delta\gamma_z > mc^2$, where $<>$ indicates an average over the electron distribution. To do this, we first note that $v_z^2 = v^2 - (v_x^2 + v_y^2)$, where v is the electron speed, $v_x = dx/dt$, $v_y = dy/dt$ and $\delta\gamma_z = \beta_z \gamma_z^3 \delta\beta_z$, where $\delta\beta_z$ is the spread in β_z. From the first of these relations it follows that $| < \delta v_z > | \approx < (v_x^2 + v_y^2) > /2v$. Next, evaluating v_x and v_y with the aid of Eqs. (15) and (16) one obtains

$$\delta\gamma_z = \frac{\gamma_z^3}{3} \left(\frac{\Omega X_b}{2c}\right)^2 \left[1 + \left(\frac{\Omega_0}{\Omega}\right)^2\right], \tag{17}$$

where it has been assumed that ξ is uniformly distributed in the interval [0,1]. This spread in energy will contribute to the inhomogeneous broadening of the radiation from the electron beam.

Equations (6), (7), (15) and (16) form a closed system of equations for the analysis of the electron dynamics of a grating FEL. They form the basis for the numerical results presented in **Sec. III**. It is useful at this point to derive the 'pendulum' equation[21] for the phase by neglecting the motion in the $x - y$ plane.

Setting $v_x = 0$, $v_y = 0$ and $\gamma = \gamma_z$, Eqs. (6) and (7) can be combined into a single equation for ψ_j:

$$\frac{d^2\psi_j}{dt^2} = -\frac{\pi|e|E_1}{\gamma_{zj}^3 md}\sinh[k_1(D - x_j)]\exp(i\psi_j) + c.c. \tag{18}$$

Equation (18) shows that the motion of an electron consists of synchrotron oscillations which, in the case of the grating FEL, take place in the potential well formed by the electric field of the spatial harmonic.

C. Radiated Power in the Small-Signal Regime

The small-signal analysis of Eq. (18) proceeds by taking E_1 and γ_z as constants and solving the equation iteratively, assuming that the right-hand side is a small term. Since this analysis is standard we shall not repeat it here. From the small-signal analysis of Eq. (18) the power radiated by an electron beam of thickness $2X_b$ passing at a distance δ above the grating is given by[13,20]

$$\frac{d\mathcal{E}_{rad}}{dt} = \frac{\omega|E_1|^2}{16}\frac{I_b[A]}{I_0}\left(\frac{L_z}{\beta_z\gamma_z}\right)^3\left[\frac{\sinh(2k_1X_b)}{2k_1X_b}\cosh[2k_1(D - X_b - \delta)] - 1\right]g(\Theta), \tag{19}$$

where $I_0 = 1.7\times10^4$, $I_b[A]$ is the beam current in Ampères, $g(\Theta) \equiv d(\sin\Theta/\Theta)^2/d\Theta$, and

$$\Theta \equiv \left(\frac{\omega}{v_z} - \frac{2\pi}{d}\right)\frac{L_z}{2}, \tag{20}$$

and L_z is the interaction length along the z axis.

D. Start-Oscillation Condition and Gain of Grating FEL

In the configuration indicated in Fig. 1 a mirror is placed above the grating to form an open resonator for the oscillator. If Q denotes the effective quality factor of the resonator, the start-oscillation condition is expressed by

$$\frac{d\mathcal{E}_{rad}}{dt} = \frac{\omega}{Q}\mathcal{E}_{rad}, \tag{21}$$

where $\mathcal{E}_{rad}$, the total radiation energy stored in the optical cavity, is given by

$$\mathcal{E}_{rad} = \frac{AD}{4\pi}\left\{E_0^2 + \sum_{n=1}^{\infty}\frac{E_n^2}{2}\left[\left(\frac{2n\pi}{k_n d}\right)^2\frac{\sinh(2k_nD)}{2k_nD} + \left(\frac{k_x}{k_n}\right)^2\right]\right\}, \tag{22}$$

where A is the cross-sectional area of the optical cavity. In writing Eq. (22) the contribution of the field energy in the grating slots has been omitted. According to our earlier assumptions only the $n = 1$ spatial harmonic is excited by the electron beam. Noting that $k_1 D \gg 1$, with the aid of Eq. (4) we identify the first term in Eq. (21) as the predominant contribution to the expression for $\mathcal{E}_{rad}$. Making use of Eqs. (4), (18), (21) and (22) one obtains an estimate for the start-oscillation current which is expressible in the form

$$I_b[A] \approx 800(-\ln R)\frac{A\lambda}{L_x^3}\frac{(\beta_z\gamma_z)^3}{\sin^2(k_xD)}\left[\frac{\pi s/d}{\sin(\pi s/d)}\right]^2\frac{2k_1X_b}{\sinh(2k_1X_b)}\exp[2k_1(X_b+\delta)]. \tag{23}$$

In writing Eq. (23) the maximum value of $g(\Theta)$, defined prior to Eq. (20), is taken to be equal to 0.54. Additionally, the effective reflectivity R of the optical cavity has been introduced by making use of the formula relating the reflectivity to the cavity quality factor,[23] i.e., $Q = \omega D/c(-\ln R)$.

As illustrative examples, Tables 1 and 2 list sets of parameters for grating FELs using a 100 kV electron beam to generate radiation at $\lambda = 100\,\mu m$ and a 1/2 MV electron beam to generate radiation at $\lambda = 10\,\mu m$. Several points should be noted in connection with these tables. First, the start-oscillation current is determined from Eq. (23) by inserting the value of k_x obtained from a solution of the dispersion relation in Eq. (5). Equation (5) generally has an infinite number of roots corresponding to all the discrete modes in the open resonator. The entries in Tables 1 and 2 indicate the lowest start-oscillation currents corresponding to the roots of Eq. (5) that fulfil the resonance condition $\lambda/d \approx 1/\beta_z$. Second, the Q value has been chosen so that the cavity fill-time is reasonably short compared to the expected duration of the electron beam pulse. Third, the relative energy spread is evaluated with the aid of Eq. (17). Fourth, The function $g(\Theta)$, defined prior to Eq. (20), is the well-known derivative of the spontaneous line shape, $(\sin\Theta/\Theta)^2$. The predominant region of gain is limited to the range $0 < \Theta < \pi$. Evaluation of $\partial\Theta/\partial\lambda$ at fixed v_z (for homogeneous broadening) allows one to estimate the spread in the wavelengths, $\delta\lambda$, of the emitted radiation. That is

$$\delta\lambda/\lambda = \beta_z(\lambda/L_z).$$

Fifth, the output power is given by $\eta I_b V$, where η is the extraction efficiency and V is the beam voltage. The extraction efficiency is obtained from the numerical results presented in **Sec. III**. Finally, the gain per pass, defined by

$$G = \frac{L_z}{v_z}\frac{d\mathcal{E}_{rad}/dt}{\mathcal{E}_{rad}},$$

is also indicated in Tables 1 and 2.

III. Extraction Efficiency : Numerical Simulations and Analytical Estimates

The extraction efficiency η, defined as the fraction of the electron beam kinetic energy that is converted into electromagnetic radiation energy, is a key figure-of-merit of any source of high-power radiation. An estimate for the extraction efficiency is obtained by considering the maximum tolerable spread, δv_z, in the axial velocity and the corresponding spread in the detuning, $|\delta\Theta|$, where Θ is defined in Eq. (20). As usual, the requirement that $|\delta\Theta|$ be less than π leads to an *upper* bound for the extraction efficiency, which can be expressed in the form

$$\eta = \frac{\lambda}{L_z}\frac{(\gamma_z^2-1)^{3/2}}{\gamma_z - 1}. \tag{24}$$

An estimate of the energy spread on the electron beam may be made by using Eq. (17). The gain in Tables 1 and 2, which is based on the model of a cold, monoenergetic beam, is achieved provided this relative energy spread is small compared to the extraction efficiency indicated in Eq. (24). The numerical results to be presented verify this assumption.

In this section we shall discuss the results for the efficiency obtained from a numerical solution of Eqs. (6), (7) and (15) for the electrons comprising the beam and compare the results with analytical estimates. In subsection **A** a 100 kV beam is used to generate 100 μm radiation and in subsection **B** a 1/2 MV beam is employed to generate 10 μm radiation. Each subsection is divided into two parts. In **i)** we discuss the example of an infinitely-thin beam (i.e., $X_b \to 0$). The

example of a finite-thickness electron beam is, of course, more important since it is closer to reality. Besides this, however, numerical simulations and analytical calculations allow us to explore and gain a deeper understanding of the nonlinear stage of the interaction. The beam with finite thickness is examined in **ii)**, with Case (a) presenting the results in the case of laminar flow and Case (b) presenting the results in the case of the beam with full transverse electron motion.

A. Radiation wavelength $\lambda = 100\,\mu m$

i) Infinitely-Thin Beam

Figure 3 (a) shows the efficiency of generation of 100 μm radiation as a function of the electric field amplitude of the fundamental spatial harmonic for a cold, *infinitely thin electron beam*. The efficiency in this case has been optimized with respect to the detuning Θ defined in Eq. (20) to obtain the maximum extraction. For the idealized case of a monoenergetic, infinitely-thin beam, space-charge effects are eliminated by using a very small beam current. Inserting the corresponding numerical values, the efficiency according to Eq. (24) is 0.72%, which is to be compared with the code result of 0.63% indicated in Fig. 3 (a).

Following Eq. (18) we have noted that the motion of the electrons in the radiation field is in the form of synchrotron oscillations in the potential well formed by the slow-wave corresponding to the $n = 1$ spatial harmonic. The saturation mechanism in this process is similar to that in the conventional FEL. That is, the maximum extraction efficiency is obtained when an electron loses all its initial kinetic energy in the potential well and, in the moving frame, its initial velocity is

reversed. The reversal in velocity is attained after a time $\sim \pi/\Omega_{syn0}$, where Ω_{syn0} is the synchrotron frequency. From Eq. (18),

$$\Omega_{syn0} = \left\{ \frac{2\pi}{d} \frac{|e|E_1}{m\gamma_z^3} \sinh[k_1(D - X_0)] \right\}^{1/2} . \tag{25}$$

In Eq. (25), X_0 is the x coordinate of the beam centroid. In the examples where the beam is taken to be infinitely-thin, X_0 is, of course, the x coordinate of the beam, i.e., the distance of the beam from the grating surface.

In optimizing the detuning Θ [defined in Eq. (20)] for an infinitely-thin beam we are, in effect, choosing the frequency ω such that the electrons at $x = X_0$ undergo $\sim 1/2$ of a synchrotron oscillation in the interaction length L_z. The discrepancy between the value for the efficiency calculated from Eq. (24) and the peak value in Fig. 3 (a) is a reflection of the fact that the electrons are somewhat smeared in the potential well in which they are trapped. Since they do not oscillate in the potential well as a 'macroparticle', we expect a reduction in the extraction efficiency compared to the the upper bound given in Eq. (24). This is consistent with our results.

ii) Finite-Thickness Beam

Case (a) Electron Beam with Laminar Flow

Figure 3 (b) shows the efficiency for a finite-thickness beam with the gyration of the electrons artificially suppressed in the numerical code. This figure indicates a peak efficiency of 0.36%, which is smaller than the value for the case of the infinitely-thin beam shown in Fig. 3 (a).

For a thick beam the synchrotron frequency varies according to the x coordinate of the electrons. Consequently the inner electrons experience a field that is larger than the optimal value and they execute more than $1/2$ of a synchrotron oscillation. The outer electrons, on the other hand, experience a smaller field than the optimal value and thus do not complete the $1/2$-synchrotron motion necessary to completely transfer their energy to the radiation field. It is simple to obtain an estimate of the factor by which the extraction efficiency is reduced. The frequency Ω_{syn0} is greater than the mean synchrotron frequency of electrons located at $x > X_0$ by

$$F_+ = \frac{\Omega_{syn0}}{< \Omega_{syn} >},$$

where

$$\Omega_{syn} = \left\{ \frac{2\pi}{d} \frac{|e|E_1}{m\gamma_z^3} \sinh[k_1(D-x)] \right\}^{1/2}, \tag{26}$$

is the synchrotron frequency of electrons at a distance x from the grating surface, Ω_{syn0} is defined in Eq. (25) and $<>$ indicates an average over the interval $X_0 \leq x \leq 2X_b$. The quantity F_+ may be viewed as the the amount by which the interaction length L_z in Eq. (24) is effectively increased, thus leading to a reduction in the extraction from the electrons located at $x > X_0$. Similarly, for electrons with $x < X_0$ the extraction is also reduced. For these electrons the mean synchrotron frequency is greater than Ω_{syn0} by

$$F_- = \frac{< \Omega_{syn} >}{\Omega_{syn0}},$$

where $< \Omega_{syn} >$ is the average, over the interval $0 < x < X_0$, of the synchrotron frequency defined Eq. (26). Considering both groups of electrons together, the

extraction efficiency is expected to be reduced, relative to the infinitely-thin beam case, by $1/F$, where

$$F = \frac{1}{2}(F_+ + F_-).$$

Inserting the appropriate values, we find $F = 1.8$. This is fairly close to the value of $0.63/0.36 = 1.7$ for the ratio of the peak efficiencies in Figs. 3 (a) and 3 (b).

Case (b) Electron Beam with Full Transverse Motion

Figure 3 (c) shows the extraction efficiency for a warm, finite-thickness electron beam ($X_b = 25\,\mu m$). (See Table 1 for other parameters in this example.) The peak efficiency indicated in Fig. 3 (c), $\eta = 0.46\%$, is observed to be smaller than the peak efficiency for the infinitely-thin beam example in Fig. 3 (a) *but higher than that for a thick beam with laminar flow.* This is an important result which we shall discuss further.

For a thick beam the synchrotron frequency varies according to the x coordinate of the electrons. As a consequence of their gyromotion, however, the electrons rotate about the beam axis and sample the transverse profile of the electric field as they cross the interaction region. This tends to restore, to some extent, the extraction to the value obtained in the case of an infinitely-thin beam. To assess the effect of electron gyration on the extraction quantitatively, Eq. (15) may be substituted into the pendulum equation, Eq. (18), to obtain

$$\frac{d^2\psi_j}{dt^2} = -\frac{\pi|e|E_1}{2\gamma_{zj}^3 md} \sum_{r=-\infty}^{\infty} I_r(k_1\xi X_b)\left[(-1)^r \exp(\Phi) - \exp(-\Phi)\right]\exp(i\psi_j) + c.c., \quad (27)$$

where $\Phi = k_1(D - X_0) + ir(\Omega t + \theta)$ and I_r is the modified Bessel function of the first kind of order r. Equation (27) may be simplified by noting that the electrons

gyrate many times as they transit the interaction region; i.e., $\Omega/\Omega_{sym0} \gg 1$, where Ω is the gyration frequency defined following Eq. (10) and Ω_{sym0} is the synchrotron frequency defined in Eq. (25). Assume that $\psi_j = \Psi_j + \delta\psi_j$, where Ψ_j is slowly varying and $\delta\psi_j$ is small and rapidly varying. Upon inserting this into Eq. (27) and averaging with respect to the rapid oscillations, we obtain

$$\frac{d^2\Psi_j}{dt^2} = -\frac{\pi|e|E_1}{\Gamma_{zj}^3 md} I_0(k_1\xi X_b)\sinh[k_1(D-X_0)]\exp(i\Psi_j) + \mathcal{O}(E_1^2) + c.c., \qquad (28)$$

where the Γ_{zj} is the slowly-varying part of the relativistic factor. Equation (28) shows that for an electron (with given $\xi > 0$) the synchrotron frequency is not identical to that for an electron located on the beam axis, i.e., the frequency given by Eq. (25). Since $I_0 > 1$, the synchrotron frequency is effectively increased by $\sqrt{I_0}$. This implies that the electron undergoes more than 1/2 of a synchrotron oscillation in the interaction length, thus transferring less energy to the radiation and reducing the overall extraction. For the beam as a whole, the extraction efficiency is expected to be reduced by $< I_0^{1/2}(k_1\xi X_b) >^{-1}$, where $<>$ indicates an average over the random variable ξ. Inserting the appropriate numerical values we find $< I_0^{1/2}(k_1\xi X_b) >= 1.24$, which is close to the ratio of the peak efficiencies in Figs. 3 (a) and 3 (c), i.e., $0.63/0.46 = 1.37$.

B. Radiation wavelength $\lambda = 10\,\mu m$

i) Infinitely-Thin Beam

Next we examine an example of $10\,\mu m$ radiation generated by a $1/2\,MV$ electron beam. Table 2 shows the parameters for this example. Again, for comparison

purposes it is useful to know the extraction efficiency for the case of the infinitely thin beam. The peak extraction efficiency in this case is 0.11%, as indicated in Fig. 4 (a), which is to be compared to the value of 0.13% as determined from Eq. (24).

ii) Finite-Thickness Beam

Case (a) Electron Beam with Laminar Flow

Figure 4 (b) shows the extraction efficiency for the case of a finite-thickness beam with the gyration of the electrons artificially eliminated. The peak efficiency is observed to be 0.068%. In this case, $F = 1.6$, which is in good agreement with the ratio of the peak efficiencies in Figs. 4 (a) and 4 (b), namely, $0.11/0.068 = 1.6$.

Case (b) Electron Beam with Full Transverse Motion

Finally, in Fig. 4 (c) we show that the extraction efficiency for the case of the finite-thickness beam with full transverse motion is 0.093%. Inserting the appropriate numerical values, we find $< I_0^{1/2}(k_1 \xi X_b) >= 1.14$, which is in close agreement with the ratio of the peak efficiencies in Figs. 4 (a) and 4 (c), i.e., $0.11/0.093 = 1.18$.

IV. Discussion and Concluding Remarks

The grating FEL has the potential of developing into a truly compact, table-top free-electron source of IR radiation. In this paper we have presented a preliminary study of a possible set of design parameters for a source utilizing a 100 kV electron beam to generate 100 μm radiation and one utilizing a $1/2$ MV beam to generate $10\,\mu m$ radiation. The design parameters have been obtained from a small-signal analysis of the pendulum equation. This equation describes the synchrotron oscillations of electrons in the slow-wave structure associated with the grating.

In this paper we emphasize the use of mildly relativistic ($\leq 1/2$ MV) beams, primarily to avoid the bulk and expense associated with multi-MV beams. This entails certain trade-offs that point to the wide latitude available in designing a grating FEL. To illustrate this, Table 3 presents an example of a 5 MV beam employed to generate 10 μm radiation. The start-oscillation current in this case is kept reasonably low by using a long-thin grating and assuming a somewhat higher effective reflectivity. Compared to the design parameters in Table 2, the 5 MV system is characterized with higher output power and gain, the strength of the guide magnetic field is relatively modest and an electron beam with a larger relative energy spread can be accommodated. As far as the nonlinear saturation is concerned, the 5 MV beam illustrates an interesting point. Although the beam is 5 wavelengths thick, the extraction efficiency is nearly equal to that for an infinitely-thin beam. This result is in quantitative agreement with the analysis presented in **Sec. III.**

The nonlinear evolution of the grating FEL has been analyzed with the aid of a particle simulation code. This code follows the motion of electrons through given fields and allows an accurate estimation of the nonlinear extraction efficiency to be made. We have made use of a novel method of following the transverse motion of the electrons in the presence of an axial guide magnetic field and the self-fields which naturally incorporates the effects associated with the finite emittance of the electron beam.

We have studied the extraction efficiency of the grating FEL in detail for three examples. The example of the infinitely-thin beam is found to have the highest extraction and the example of a thick beam with laminar flow is found to have the smallest extraction. We have found the remarkable result that for a thick beam, gyration of the the electrons about the beam axis leads to an enhancement of the extraction efficiency as compared to the case with laminar flow. This is due to the fact that electron gyration tends to effectively reduce the variation of the slow-wave electric field normal to the grating surface.

Acknowledgment

The authors are grateful to Drs. A. Fisher, A. W. Fliflet, S. H. Gold and W. M. Manheimer for valuable discussions. This work was supported by the Defense Sciences Office at DARPA and by the Office of Naval Research.

References

[1] S. J. Smith and E. M. Purcell, Phys. Rev. 92, 1069 (1953).

[2] F. S. Rusin and G. D. Bogomolov, Zh. Eksp. Teor. Fiz. Pis'ma 4, 236 (1966). [JETP Lett. 4, 160 (1966).]

[3] F. S. Rusin and G. D. Bogomolov, Proc. IEEE 57, 720 (1969).

[4] V. K. Korneenkov, A. A. Petrushin, B. K. Skrynnik and V. P. Shestopalov, Izv. Vyssh. Uchebn. Zaved. Radiofiz. 20, 290 (1977). [Radiophys. Quantum Electron. 20, 197 (1977).]

[5] I. D. Revin. B. K. Skrynnik, A. S. Sysoev, O. A. Tret'yakov and V. P. Shestopalov, Izv. Vyssh. Uchebn. Zaved. Radiofiz. 20, 764 (1977). [Radiophys. Quantum Electron. 20, 524 (1977).]

[6] A. I. Tsvyk, Izv. Vyssh. Uchebn. Zaved. Radiofiz. 21, 1216 (1978). [Radiophys. Quantum Electron. 21, 850 (1979).]

[7] V. K. Korneyenkov and V. P. Shestopalov, Radiotekhnika i Electronika 22, 412 (1977). [Radio Eng. Electron Phys. 22, 148 (1977).]

[8] E. I. Nefëdov, Izv. Vyssh. Uchebn. Zaved. Radiofiz. 20, 1740 (1977). Radiophys. Quantum Electron. 20, 1198 (1977).

[9] M. B. Tseytlin, G. A. Bernashevskiy, V. D. Kotov and I. T. Tsitson', Radiotekhnika i Elektronika 22, 1515 (1977). [Radio Eng. Electron Phys. 22, 132 (1977).]

[10] I. M. Balaklitskii, G. S. Vorob'ev, A. I. Tsvyk and V. P. Shestopalov, Izv. Vyssh. Uchebn. Zaved. Radiofiz. 21, 1853 (1978). [Radiophys. Quantum Electron. 21, 1289 (1979).]

[11] A. S. Bakai, K. A. Lukin and V. P. Shestopalov, Izv. Vyssh. Uchebn. Zaved. Radiofiz. 22, 1117 (1979). Radiophys. Quantum Electron. 22, 774 (1980).]

[12] K. Mizuno and S. Ono, in *Infrared and Millimeter Waves*, (Academic, New York, 1979), vol. 1, p. 213.

[13] J. M. Wachtel, J. Appl. Phys. 50, 49 (1979).

[14] D. E. Wortman, R. P. Leavitt, H. Dropkin and C. A. Morrison, Phys. Rev. A24, 1150 (1981).

[15] F. J. Crowne, R. P. Leavitt and T. L. Worchesky, Phys. Rev. A24, 1154 (1981).

[16] D. E. Wortman, H. Dropkin and R. P. Leavitt, IEEE J. Quantum Electron. QE-17, 1333 (1981); IEEE J. Quantum Electron. QE-17, 1341 (1981).

[17] D. E. Wortman and R. P. Leavitt, in *Infrared and Millimeter Waves*, (Academic, New York, 1983), vol. 7, p. 321.

[18] E. M. Marshall, P. M. Phillips and J. E. Walsh, IEEE Trans. Plasma Sci. 16, 199 (1988).

[19] E. Garate, R. Cherry, A. Fisher and P. Phillips, J. Appl. Phys., 64, 6618 (1988).

[20] J. E. Walsh, T. L. Buller, B. Johnson, G. Dattoli and F. Ciocci IEEE J. Quantum Elec. QE-21, 920 (1985).

[21] W. B. Colson, Phys. Lett. A, 64, 190 (1977).

[22] J. D. Lawson, *The Physics of Charged-Particle Beams*, (Oxford University Press, Oxford, 1978), chap. 4.

[23] A. Yariv, *Quantum Electronics*, (Wiley, New York, 1989), sec. 7.4.

Table 1: Design parameters for a grating FEL Oscillator operating at 100 μm using a 100 kV electron beam.

Wavelength λ	100	μm
Voltage V	100	kV
Current I_b	125	mA
Output Power	57.5	W
Gain/Pass G	4	%
Extraction Efficiency η	0.46	%
Interaction Length L_z	2	cm
Guide Magnetic Field B_0	3	T
Beam Thickness $\sigma_x = 2X_b$	50	μm
Beam-Grating Gap δ	0	μm
Grating Period d	55	μm
Groove Width s	27.5	μm
Groove Depth b	27.5	μm
Grating-Mirror Separation D	1	cm
Cavity Cross-Sectional Area A	1	cm^2
Effective Reflectivity R	99	%
Cavity Quality Factor Q	6×10^4	
Relative Energy Spread $\delta\gamma_z/(\gamma - 1)$	0.2	%
Relative Wavelength Spread $\delta\lambda/\lambda$	0.3	%

Table 2: Design parameters for a grating FEL Oscillator operating at 10 μm using a 1/2 MV electron beam.

Wavelength λ	10	μm
Voltage V	1/2	MV
Current I_b	400	mA
Output Power	186	W
Gain/Pass G	47	%
Extraction Efficiency η	0.093	%
Interaction Length L_z	4	cm
Guide Magnetic Field B_0	10	T
Beam Thickness $\sigma_x = 2X_b$	10	μm
Beam-Grating Gap δ	0	μm
Grating Period d	9	μm
Groove Width s	4.5	μm
Groove Depth b	4.5	μm
Grating-Mirror Separation D	1	mm
Cavity Cross-Sectional Area A	1	cm^2
Effective Reflectivity R	99	%
Cavity Quality Factor Q	6×10^4	
Relative Energy Spread $\delta\gamma_z/(\gamma - 1)$	0.03	%
Relative Wavelength Spread $\delta\lambda/\lambda$	0.02	%

Table 3: Design parameters for a grating FEL Oscillator operating at 10 μm using a 5 MV electron beam.

Wavelength λ	10	μm
Voltage V	5	MV
Current I_b	100	mA
Output Power	3	kW
Gain/Pass G	81	%
Extraction Efficiency η	0.61	%
Interaction Length L_z	16	cm
Guide Magnetic Field B_0	1	T
Beam Thickness $\sigma_x = 2X_b$	50	μm
Beam-Grating Gap δ	0	μm
Grating Period d	10	μm
Groove Width s	5	μm
Groove Depth b	5	μm
Grating-Mirror Separation D	1	mm
Cavity Cross-Sectional Area A	1	cm^2
Effective Reflectivity R	99.5	%
Cavity Quality Factor Q	1.3×10^5	
Relative Energy Spread $\delta\gamma_z/(\gamma - 1)$	0.5	%
Relative Wavelength Spread $\delta\lambda/\lambda$	6.2×10^{-3}	%

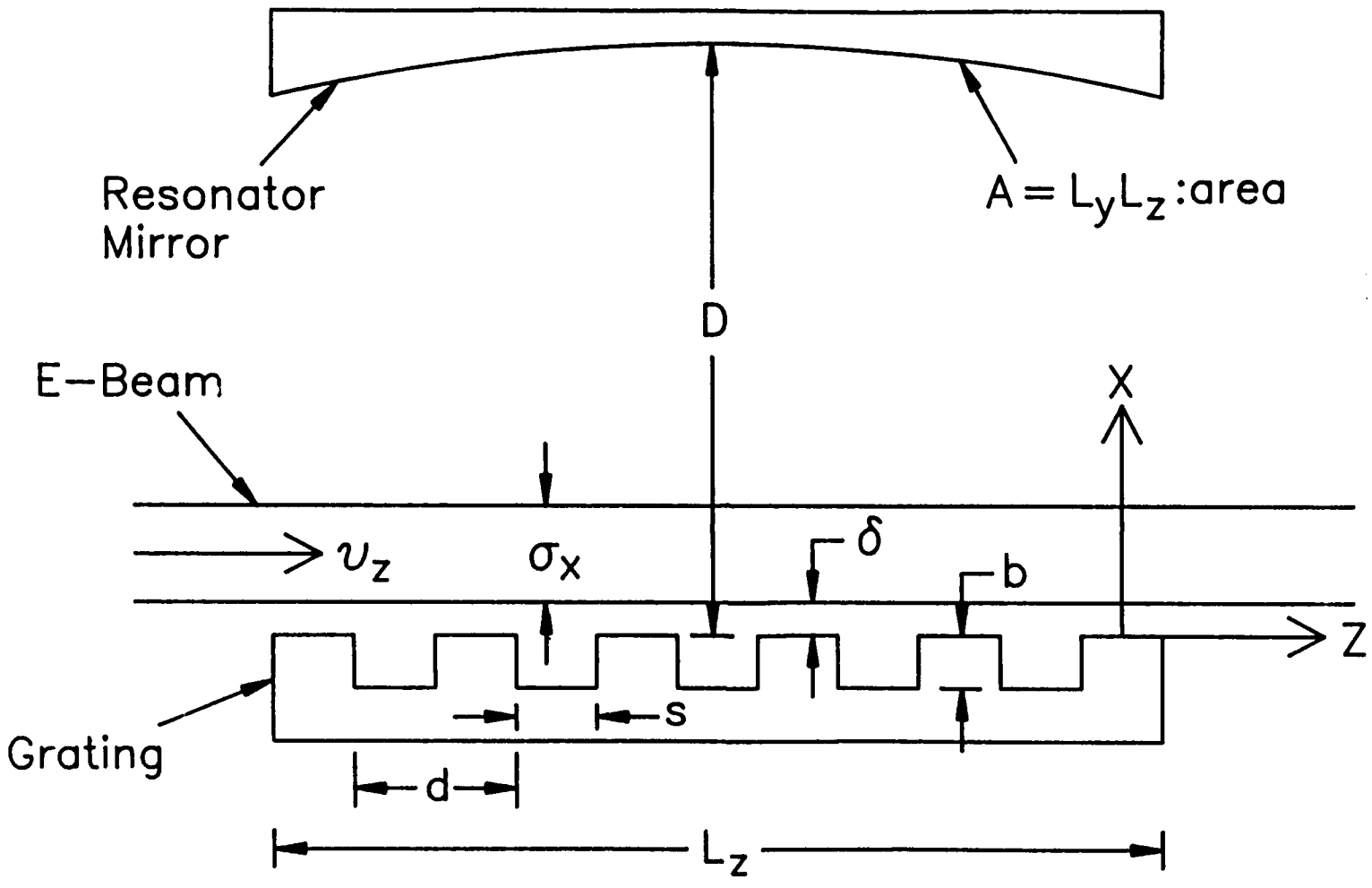

Figure 1: Schematic of an open resonator configuration for a grating FEL oscillator. Space between upper mirror and upper surface of grating is referred to as region I; region II refers to the slots in the grating.

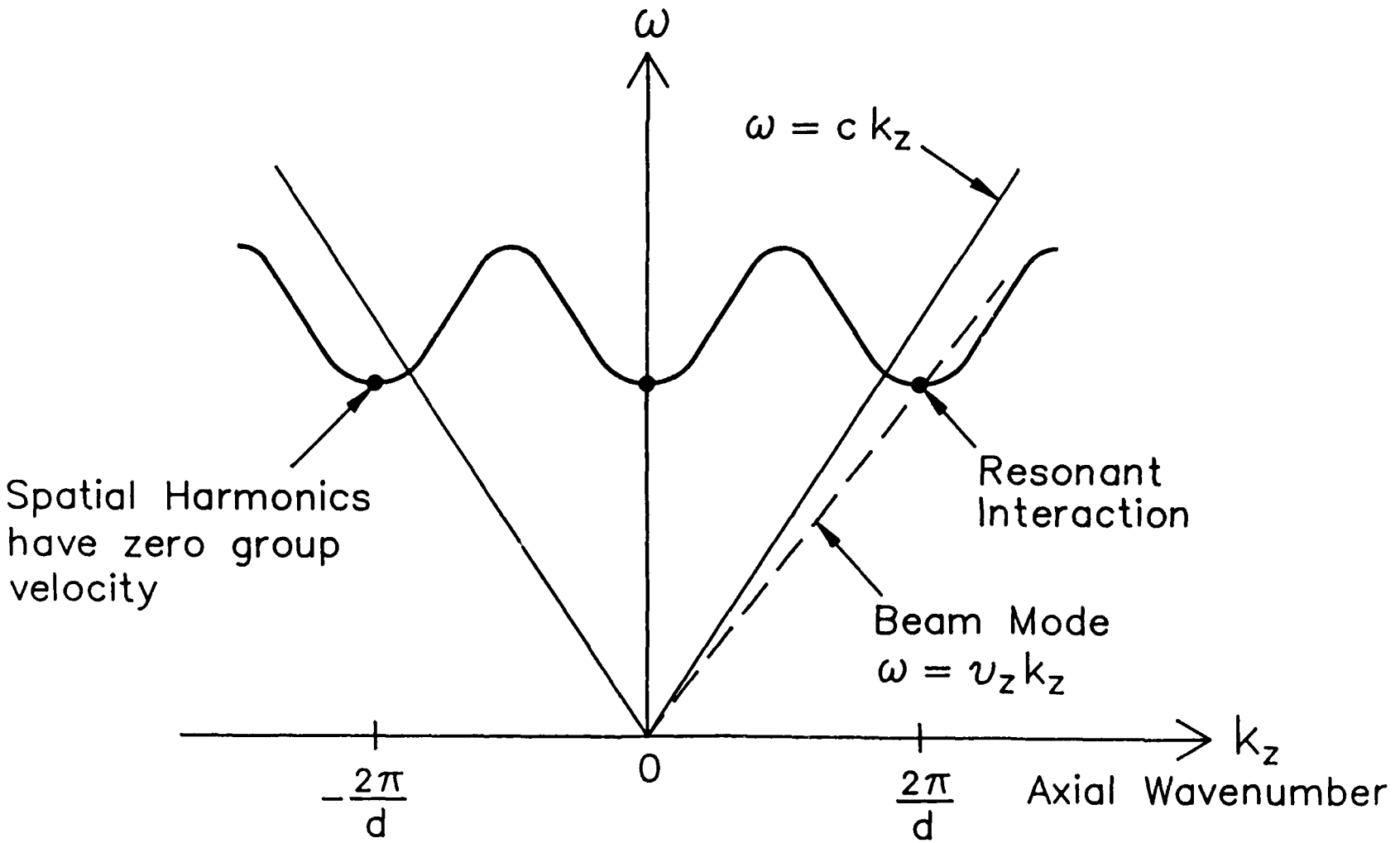

Figure 2: Schematic of a dispersion curve for the grating FEL oscillator in Fig. 1. The axial wavenumber is denoted by k_z.

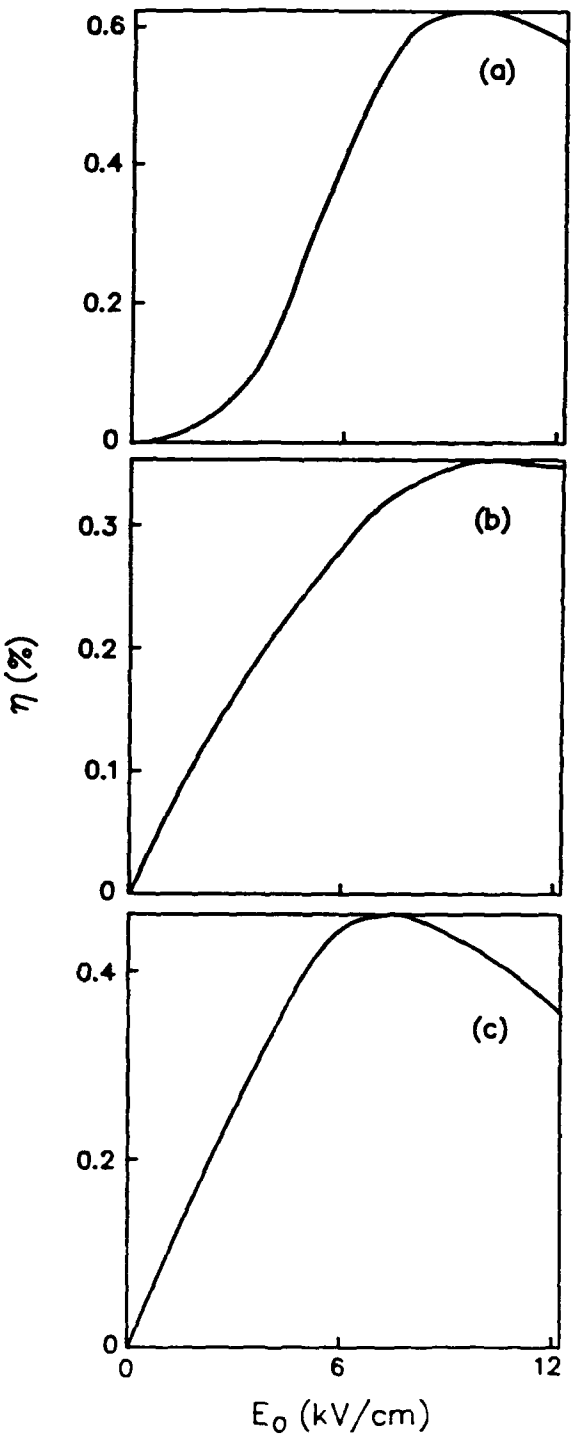

Figure 3: Extraction efficiency, η, versus amplitude of fundamental spatial harmonic, E_0, for $\lambda = 100\,\mu m$ radiation using a 100 kV beam. Beam axis is 25 μm above grating surface. (a) Infinitely-thin beam. (b) Finite-thickness beam with laminar flow ($X_b = 25\,\mu m$). (c) Finite-thickness beam with full transverse motion ($X_b = 25\,\mu m$).

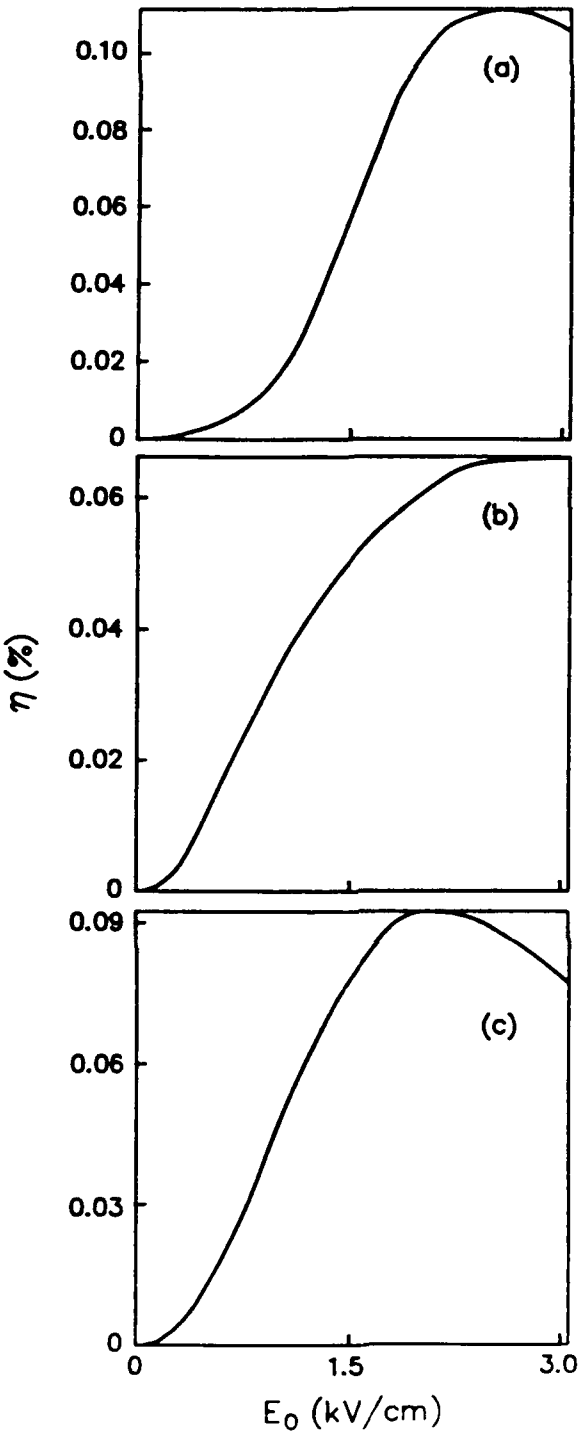

Figure 4: Extraction efficiency, η, versus amplitude of fundamental spatial harmonic, E_0, for $\lambda = 10\,\mu m$ radiation using a $1/2$ MV beam. Beam axis is 5 μm above grating surface. (a) Infinitely-thin beam. (b) Finite-thickness beam with laminar flow ($X_b = 5\,\mu m$). (c) Finite-thickness beam with full transverse motion ($X_b = 5\,\mu m$).